American Mineralogist, Volume 78, pages 1117–1134, 1993

Magma transport and metasomatism in the mantle: A critical review of current geochemical models

J. E. Nielson, H. G. Wilshire
U.S. Geological Survey, 345 Middlefield Road, M.S. 975, Menlo Park, California 94025, U.S.A.

Abstract

Conflicting geochemical models of metasomatic interactions between mantle peridotite and melt all assume that mantle reactions reflect chromatographic processes. Examination of field, petrological, and compositional data suggests that the hypothesis of chromatographic fractionation based on the supposition of large-scale percolative processes (Navon and Stolper, 1987) needs review and revision. In the hypothesis, melts develop enrichment fronts of incompatible elements as the melt percolates through a porous mantle column of refractory peridotite composition and imprint the fractionation patterns on peridotite elsewhere.

Current models that use Navon and Stolper's (1987) chromatographic fractionation concept are applied to rocks of the Lherz and Horoman massifs. The calculations produce poor or limited results for the sequence of compositional variations in time and space, and the assumptions do not accord with field relations and estimates of mantle conditions from experiments. In the Lherz model, modest LREE enrichments require melt percolation for as long as 25000 yr, an unrealistic life span for mantle dike conduits that supply metasomatizing melts. Continuous porous flow of melts also requires host peridotite temperatures at or above the liquidus.

Models of regional pervasive porous flow conflict with structural and seismic evidence that fractures control fluid transportation in the upper mantle. Effects of porous-medium flow have been inferred in studies of mantle peridotite samples on scales of tens of meters at most, but are well documented only on scales of centimeters or decimeters. In all these hypotheses, porous flow is fundamentally controlled by proximity to magma-filled fractures.

Well-constrained rock and mineral data from xenoliths indicate that many elements that behave incompatibly in equilibrium crystallization processes are absorbed immediately when melts emerge from conduits into depleted peridotite. After reacting to equilibrium with the peridotite, melt that percolates away from the conduit is largely depleted of incompatible elements. Continued addition of melts extends the zone of equilibrium farther from the conduit. Such a process resembles ion-exchange chromatography for H_2O purification, rather than the model of chromatographic species separation proposed by Navon and Stolper (1987).

Introduction

Debate about the scale of mantle metasomatism has been ongoing for two decades. Early speculative hypotheses identified cryptic mantle metasomatism as a regional-scale process in contrast to demonstrably local modal metasomatism (Harte, 1983). Formation of harzburgite on a regional scale was postulated to result from dissolution of clinopyroxene due to pervasive melt infiltration of lherzolite (Kelemen et al., 1992), and regional formation of biotite pyroxenite was ascribed to metasomatic conversion of peridotite (Lloyd et al., 1987; Dawson and Smith, 1992). These hypotheses are essentially untestable, but recent studies of massifs and xenoliths promise to give us a better framework for understanding both the scales and processes of mantle metasomatism.

We have long studied composite mantle xenoliths and also have made field observations and petrologic studies of the Lherz and other massifs. Our purpose in this paper is to point out problems inherent in current geochemical models that assume large-scale infiltration (percolation) processes. We question some interpretations of the processes that formed the observed geochemical patterns and the inferred scales and consequences of those processes. By doing so, we hope to focus debate on whether the models support or prove a priori assumptions of broad scale porous-medium flow in the upper mantle, compared with magma transfer through fractures, accompanied by infiltration of wall rocks. We again emphasize the similarity of rock types, contact relations, and reactions between massifs and xenolith suites (Wilshire and Pike, 1975).

Extraction and infiltration of magma are two sides of

0003–004X/93/1112–1117$02.00

the same coin, and either or both can involve flow through a porous medium. Melts form when a portion of the mantle exceeds the solidus temperature by progressive heating or depressurization, and the melts may percolate some distance before finding or creating a fracture and opening a conduit (e.g., Nicolas, 1986; Rabinowicz et al., 1987; Wilshire and Kirby, 1989). Theoretical considerations suggest that the asthenosphere is a region of melting and melt percolation; however, abundant field evidence in alpine massifs and ophiolites and data from mantle xenoliths indicate that large volumes of magma are transmitted through the upper mantle in fractures. Metasomatic compositional gradients adjacent to magma conduits clearly show that melts react with and infiltrate wall rock (e.g., Wilshire and Shervais, 1975; Irving, 1980; Wilshire et al., 1988; Nicolas, 1989, 1990; O'Reilly et al., 1991; Nielson et al., 1993). These processes may affect relatively large volumes of the upper mantle by repetition.

Models of mantle processes that assume large-scale percolation use an analogy drawn by Navon and Stolper (1987) between mantle processes and chromatographic fractionation in laboratories to explain observed compositional variations in mantle rocks (e.g., Bodinier et al., 1990; Vasseur et al., 1991; Takazawa et al., 1992). In those models, elements (mostly REE) are thought to become separated in a melt as a result of partitioning reactions while the melt percolates distances between 1 m and 1 km through a column of mantle matrix. The melts impose their fractionated patterns on volumes of depleted mantle somewhere along the percolation path.

Mantle models are difficult to constrain because, in most cases, the original compositions of melt and matrix are uncertain. If the natural samples have been subjected to relatively few identifiable episodes of whatever processes operate in the mantle, simple experimental or theoretical models may be applicable and subject to constraints. However, samples that have undergone numerous events, involving similar or different processes, are likely to produce equivocal or misleading evidence for testing models. We can attest that even a relatively simple, well-documented single-stage metasomatic event cannot be fully constrained (Nielson et al., 1993). Therefore, the context and characteristics of the samples studied are critical elements of models of mantle processes and will limit the application of simple model assumptions.

Melt and fluid transport in the mantle

Current models of mantle metasomatism differ fundamentally in basic assumptions about melt transport mechanisms that operate in the directly observable parts of the mantle, as well as about the processes of melt-mantle interaction related to the contrasting modes of transport. Compositional models that use the Navon and Stolper (1987) hypothesis of chromatographic fractionation assume porous-medium flow through substantial distances. Models based on fracture-controlled movement of melts, with limited porous-medium flow, also use concepts of chromatographic interaction between melt and peridotite but with different boundary conditions. Both hypotheses are consistent with the possibility of porous-medium flow over large distances in the asthenosphere, where the peridotite is above solidus temperature.

Porous-medium flow

Substantial experimental and theoretical studies have focused on the factors that influence the degree of permeability in partly melted peridotite. Such factors include melt fraction and dihedral (wetting) angle (e.g., Waff and Bulau, 1982; Watson, 1982; Toramaru and Fujii, 1986; Walker et al., 1988) and the possible presence of free C-O-H fluids in the mantle (e.g., Eggler and Holloway, 1977; Wyllie, 1978; Watson and Brenan, 1987; Eggler, 1987; Watson et al., 1990). Low dihedral angles are shown by mafic and ultramafic melt compositions in peridotite at upper mantle T and P, which favor interconnection of intergranular melts and indicate the most likely conditions for porous-medium flow. Driving forces that may direct the flow of intergranular melts include melt buoyancy and deformation in upwelling mantle and rising diapirs (Stolper et al., 1981; Ribe, 1985; Nicolas, 1986, 1989, 1990; Rabinowicz et al., 1987), compaction (McKenzie, 1984), local pressure gradients (Sleep, 1988; Takahashi, 1992), and reduction of interfacial energy (Watson, 1982; Riley and Kohlstedt, 1990). Except under restricted conditions (ambient temperature near the peridotite solidus), H_2O and CO_2 have high dihedral angles in dunite, a fact that suggests the mantle may be effectively impermeable to fluids that are rich in these components (Watson et al., 1990).

Studies of natural peridotites have led to conflicting conclusions about the transmission of mafic melts through the mantle. Waff and Holdren (1981) examined dunite and lherzolite xenoliths from several localities and concluded that refractory mantle may be effectively nonporous to mafic magma. In contrast, experimental studies using pure olivine samples (Waff and Faul, 1992) were interpreted as indicating substantial grain-edge wetting by mafic melt, where the melt fraction is $>1\%$ in a rock with preferred olivine grain orientation. Thus, in mantle regions where peridotite is anisotropic, substantial permeability to mafic melts may be possible.

Experiments by Toramaru and Fujii (1986) on lherzolite indicated that dihedral angles were significantly smaller for melt in contact with olivine-olivine boundaries than for olivine-pyroxene and pyroxene-pyroxene boundaries. They concluded that the modal proportion of olivine and grain size are the most important determinants of mafic melt connectivity behavior; higher olivine contents and smaller grain sizes favor connectivity. Evidence supporting this conclusion was reported by Bussod and Christie (1991).

Experiments by Fujii et al. (1986) on synthetic peridotite powders showed that melt connectivity in dry matrix is lowered by the presence of orthopyroxene. However, connectivity in orthopyroxene-bearing rocks may increase in the presence of greater melt fractions or higher

H_2O contents of the melt. Experiments by Daines and Kohlstedt (1993) showed no difference in melt migration between olivine samples with 20 and 0% orthopyroxene. Field observations indicating selective formation of dunite at the expense of pyroxene-rich bands (Quick, 1981) also do not support a significant effect of orthopyroxene content.

Melt transport in fractures

Numerous field-oriented studies of alpine massifs, ophiolites, and xenoliths demonstrate that a common mode of melt transport in the upper mantle is in conduits formed by hydraulic fracturing (also called hydrofracturing and extensional fracturing). Nicolas (1986, 1989, 1990) modeled the earliest segregation of melts from field evidence. He suggested that melts in a mantle diapir migrate by porous flow over distances of a few centimeters and converge into small fluid-assisted gash fractures. Such fracturing occurs even in rocks with large melt fractions (Shaw, 1980); the process is generally accompanied by plastic deformation.

The process of hydraulic fracturing in the mantle requires melt pressures in excess of the peridotite yield stress, which is estimated by Nicolas (1986) to be <50 MPa. The yield stress is exceeded when the column of connected (intergranular) melt attains a height on the order of 10 km (hydrostatic pressure gradient in the melt of 5 MPa/km). At this stage melt extraction is dominated by hydraulic fracturing, even in peridotite that contains a large melt fraction (Nicolas, 1990). Various assessments suggest that, when compared with porous flow driven by a dynamic pressure gradient (matrix deformation, cf. Sleep, 1988), hydraulic fracturing and transport through fractures is more effective for transporting melts than porous flow where the vertical dimensions of the system exceed a few meters or tens of meters (Phipps-Morgan, 1987; Nicolas, 1990).

Gravity-driven porous flow is more difficult to assess in comparison with fracture transport of fluids because mechanisms that could induce large-scale permeability are poorly understood (Navon and Stolper, 1987; Nicolas, 1990). According to the model of Nicolas, conditions favoring porous flow on scales larger than ~100 m occur at depths below the column height needed for hydraulic fracturing and also in the few hundred meters below the Moho, where diapiric flow diverges horizontally and melt fractions are high. Because fracturing is a necessary condition for entrainment of xenoliths, this model implies that only the uppermost of possible porous flow zones would be sampled by xenolith-bearing magmas. However, xenoliths representing the probable uppermost mantle commonly show intensive fracturing on the scale of centimeters and dike emplacement on scales of centimeters and larger (Wilshire and Kirby, 1989), rather than the porous flow that Nicolas's model permits and which is observed in some ophiolite peridotites (Nicolas, 1989). Direct evidence of porous flow phenomena in xenoliths from the uppermost mantle is related to infiltration of melts from dikes into their wall rocks (e.g., O'Reilly et al., 1991; Wilshire et al., 1991), and indirect evidence is provided by Smith et al. (1991, 1993).

Active volcanic areas also provide evidence for hydraulic fracturing in the mantle. From detailed geologic and seismic records for Kilauea, Ryan (1988) inferred that a system of numerous concentrically arranged dikes extends beneath the volcano to a 38-km depth. In accord with earlier models of Shaw (1980), the lateral extent of the hydraulic fracturing zone is oval-shaped, with the long axis between 10 and 15 km and a mean short axis of about 6 km. During periods of low to moderate magma discharge, only the core of the conduit system is used, and outlying dikes may individually stagnate. In the zone of fracturing, bursts of seismicity about 2–3 km in diameter and 3–4 km high identify hydraulically disconnected dike systems that are likely to stagnate (Ryan, 1988). These tightly columnar sets of seismic signals are displaced from the main conduit region (Ryan, 1988, his Fig. 21).

Consistent with seismic evidence elsewhere, the conditions and observed phenomena beneath Hawaii favor hydraulic fracturing in the mantle to depths of about 60 km (cf. Nicolas, 1986). Bursts of long-lived harmonic tremors characterize a belt about 20 km wide, which extends a lateral distance of 80 km at depths between 40 and 60 km beneath Loihi, Kilauea, and Mauna Loa volcanos. The seismic signature of this belt indicates releases of large melt volumes through hydraulic fracture systems (M. P. Ryan, 1993 personal communication).

Models of fluid-mantle interactions

Chromatographic mantle hypothesis of Navon and Stolper

Navon and Stolper (1987) examined the possible consequences of reactions between enriched melts percolating long distances through relatively depleted mantle. They proposed that elements would fractionate in the percolating melts by chromatographic processes analogous to laboratory methods in which similar species are separated. In both laboratory and mantle processes, separations occur because of reactions between matrix in the column and the fluid moving through it (Fig. 1a; cf. Samuelson, 1953; Helferrich, 1962; Ritchie, 1964). Navon and Stolper (p. 286) state: "... as [the fluid] flows upward, it interacts with the matrix and trends toward equilibrium with the initial matrix [composition]. After a time the column becomes 'dirty' or 'used up' and the fluid introduced at the base passes through the column with no interaction." As fluid interacts with matrix, "each element behaves differently ... and hence fractionation can occur.... Properties of interest are assumed to change over a length scale that is large compared with the matrix grain size."

Both in laboratory processes and by the scheme of Navon and Stolper, the properties of interest governing chromatographic fractionation are the equilibrium par-

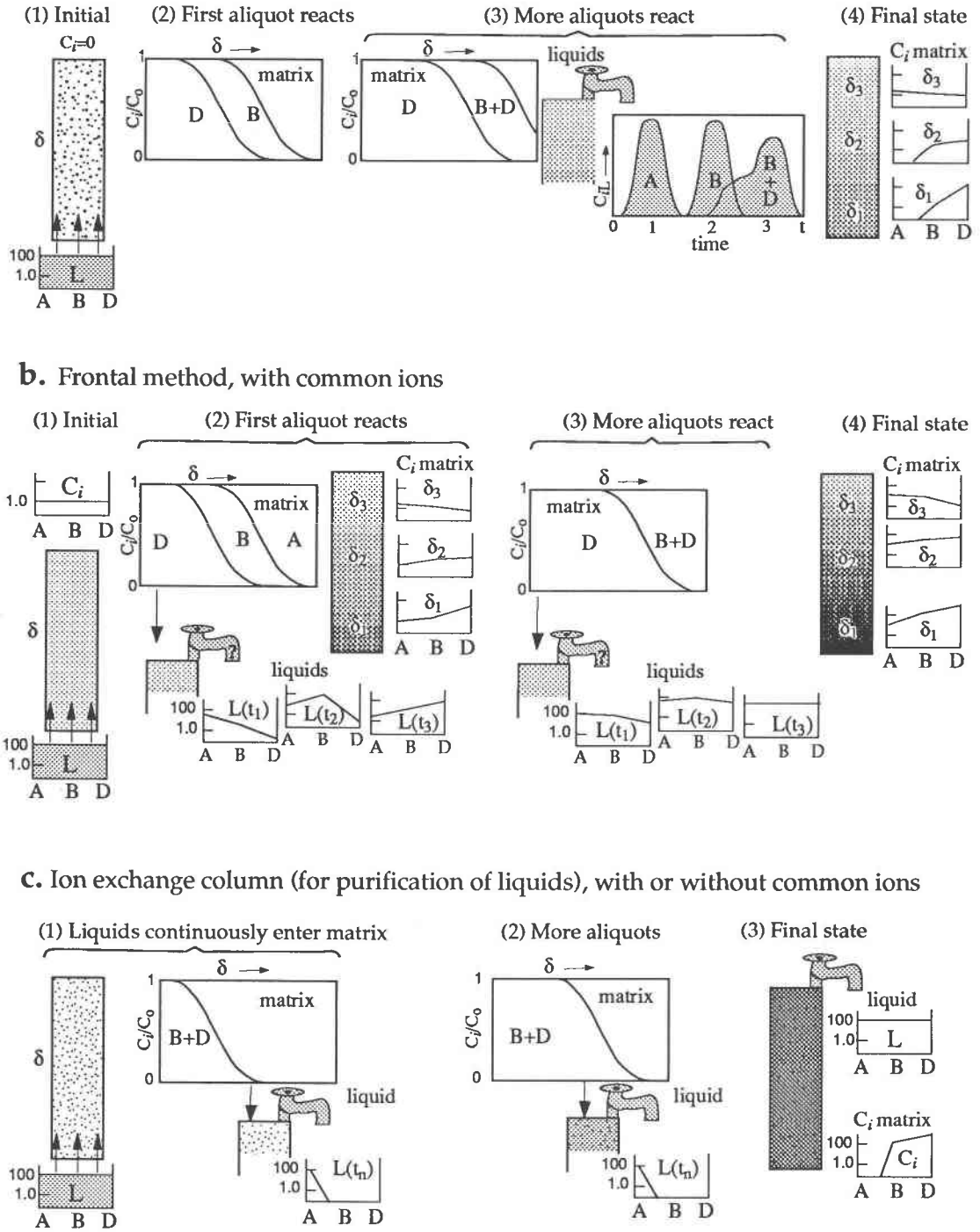

tition coefficient (K_d, matrix to melt) and the equilibrium mass fraction of an element in the liquid, X_f, which relates bulk properties of melt and matrix and includes the factor $1/K_d$ (Navon and Stolper, 1987, Eq. 2, p. 287). Compatible elements react with the matrix before incompatible elements and thus move through the column at a lower rate (Fig. 1; D is the most compatible species, A is the most incompatible). In the laboratory, a column matrix is selected for compatibility and incompatibility relations toward the species to be separated. With respect

Fig. 1. Sketch illustrating chromatographic processes. Compatibility of species (i) is in the order: A < B < D. Liquids shown entering column at base because natural percolative processes may not be gravity driven. (**a**) Frontal or breakthrough laboratory method, no common ions. (1) Volumes of solution (composition L) pass through ideal matrix (composition C_o), which contains no species to be separated ($C_i = 0$). Quantitative separation of A and B requires that A is highly incompatible relative to matrix and to B. (2) Reaction fronts shown as concentration of each species compared with original matrix (C_i/C_o), plotted against percolation distance (δ). (3) After several aliquots of mixture enter matrix, reaction front of compatible species (D) gains on B. This happens quickly, and so quantitative separation of B and D in the emerging liquid (C_{iL}) is rarely achieved (Helferrich, 1962). (4) Matrix compositions (C_i) in final state: zone δ_1 no longer has the potential to exchange or sorb D; it expands if additional liquid enters the column. Depending on actual values of exchange potentials (K_d), some quantity of B and A will be sorbed by or held in matrix at end of column (δ_2, δ_3) but may not become concentrated in matrix unless the fractionated liquid is trapped in the column. (**b**) Frontal method with common ions (direct analogy to mantle process). (1) Solid and liquid both shown with unfractionated A, B, D content; liquid (L) is enriched 100× over matrix (C_i). (2) One aliquot of liquid enters column, matrix preferentially exchanges or sorbs D, with the result that species form steep reaction fronts in matrix in 1, above. Liquids involved in a mantle process are not observed (? on faucet); L(t_1) should be enriched in species A, L(t_2) in B, and L(t_3) in D. Compositions of matrix (C_i) vary because species D accumulates to equilibrium with the liquid composition L behind the reaction front (zone δ_1). Depending on K_d values, species A and B accumulate in zones δ_3 and δ_2, respectively, where they are concentrated in liquid. (3) More aliquots of liquid L enter column and reaction front of species D moves through matrix. A is still enriched over other species in liquid L(t_1), but B and D also increase because the capacity of matrix to exchange these species is reduced by earlier reactions. Last liquids, L(t_3), pass through matrix unchanged. (4) The δ_1 represents pattern of A, B, and D when matrix reaches equilibrium with liquid, L, at reaction conditions. Equilibrium concentrations of D moved through column in same direction as liquid, but matrix first reached equilibrium with A and B in zones δ_3 and δ_2, respectively, then moved back through column to δ_1. If enough liquid reacts, all matrix in the column will achieve composition of δ_1, and no longer react with liquid L. (**c**) Ion-exchange for liquid purification (H_2O softeners); process evolves the same whether or not matrix contains common ions. (1) As aliquots of liquid L enter matrix, unwanted species (B, D) are removed by exchange with matrix and concentrate behind the reaction front. Liquids L(t_n) contain all or most of desired species (A). (2) More aliquots of liquid continue to react; reaction front moves through matrix, and liquid extracted has same composition as in Fig. 3a. (3) Reaction front expands to full length of column, which can no longer exchange B and D, and liquid L passes through unchanged. Species A never becomes significantly concentrated in matrix.

←

to a mantle process, Navon and Stolper (1987) defined compatible elements as having high K_d relative to peridotite and low X_f values; for a specific melt composition and volume ratio reacting in the mantle column, a low value of X_f is due to the high K_d.

The mantle chromatographic column discussed by Navon and Stolper (1987) is peridotite depleted in light rare-earth elements (REE) relative to chondrites ($LREE_{cn}$ of 0.008–0.03), which resembles relatively refractory compositions of harzburgite or lherzolite that are widely believed to represent samples of mantle lithosphere. Liquids (for example, silicate melts produced in the asthenosphere or volatile fluids from melting of a subducted slab) might be enriched in LREE relative to chondrites, like the composition postulated by Navon and Stolper (1987). Theoretical values of K_d and X_f used by Navon and Stolper predict that relatively compatible middle or heavy REE (HREE) will be retained in the matrix to a greater degree than incompatible LREE, and they stated, "After small quantities of melt pass through the column, the fronts of the more incompatible, light REE reach the top" of the mantle column ahead of the more compatible REE and "the matrix in this region develops U-shaped $REE_{[cn]}$ patterns. . . ." Thus, relative to other REE, the LREE should increase in the infiltrating melt.

Laboratory processes

The most common laboratory methods used to separate a suite of ions or other species introduce the species to the column in a small volume of reactive solvent. The initial reactions separate species based on K_d, as discussed above (sorption step, cf. Samuelson, 1953). Large volumes of a different liquid (elutriant), commonly an acid of a normality different from the original solution and that contains none of the solute to be separated, is used to flush the column. Species are removed in an effluent that emerges at the end of the column. Species of low K_d have a low potential to exchange with the matrix and move quickly through the matrix, whereas solutes of progressively higher K_d move at progressively slower rates through the column. Each may be collected separately in sequential aliquots of effluent, given large enough differences of K_d values, large volumes of elutriant, and a long enough column (cf. Helferrich, 1962; Ritchie, 1964).

The frontal or breakout method (Samuelson, 1953; Helferrich, 1962; Fig. 1a), in which the same solvent introduces and carries the species, more closely resembles the mantle chromatographic process hypothesized by Navon and Stolper (1987). For small volumes of solvent, the compatible species are extracted in the matrix, and the most highly incompatible species is effectively separated into the first aliquots of effluent at the end of the column (shown as the top of the column in Fig. 1a). The compatible species accumulate quickly in the matrix if larger volumes of solution enter the column. As noted by Navon and Stolper (1987; extract quoted above), the reacting matrix reaches equilibrium with the solution and loses the potential to exchange compatible elements, which therefore move farther through the column. If enough

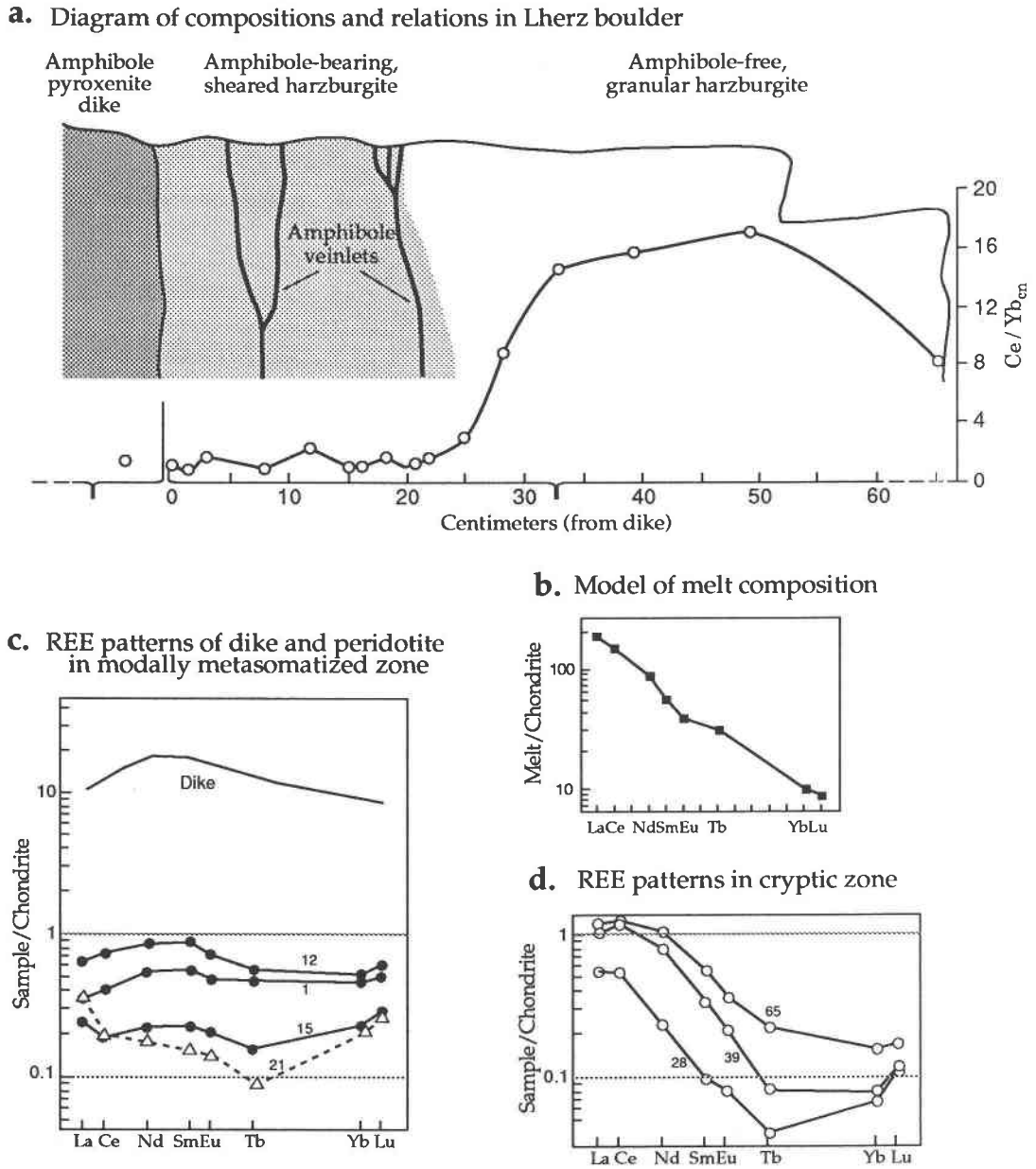

Fig. 2. Diagram and data for the Lherz boulder, basis of the Bodinier et al. (1990) metasomatic models. (**a**) Diagram of the Lherz talus block adapted from Figs. 1 and 8 of Bodinier et al. (1990, p. 599, 610). Distance from the dike contact plotted on abscissa corresponds to sample numbers. Except for the Yb content of sample 12, values of Ce/Yb_{cn} are recalculated from tables using chondrite normalization factors of Anders and Ebihara (1982). (A Yb_{cn} value for sample 12 was estimated from Fig. 6 of Bodinier et al., because the tabulated value produces Ce/Yb_{cn} 10× greater than shown by Bodinier et al., in their Fig. 8.) (**b**) Assumed REE_{cn} pattern of melt that reacted with harzburgite between 0 and 21 cm from the dike contact. This is the theoretical composition of melt in equilibrium with amphiboles of amphibole-bearing dikes from Lherz and Freychinède. (**c**) REE_{cn} patterns of Lherz subsamples, showing dike composition and range of chondrite-normalized patterns for samples in the amphibole-bearing zone. The U-shaped pattern of amphibole-bearing sample 21 is not ascribed to chromatographic fractionation by percolation but is very close to that of sample 25 (not shown) in the amphibole-free zone (Bodinier et al., 1990, their Fig. 1). (**d**) REE_{cn} patterns of subsamples in amphibole-free harzburgite. Dotted horizontal lines show correspondence between compositional ranges of samples in amphibole-bearing and amphibole-free zones. Compared with amphibole-bearing harzburgite, these sample patterns have slightly enriched $LREE_{cn}$, slightly depleted $HREE_{cn}$, and marked depletion of some middle REE.

solution is introduced into the column, all the matrix loses the potential to exchange compatible elements, and the liquid then passes through unchanged.

The goal of laboratory processes is quantitative separation of species. Therefore, a real laboratory exchange column ideally contains no ions in common with the solution. Moreover, compared with the compatible species, only very small amounts of incompatible species carried in the liquid are likely to remain in the matrix. By contrast, in the mantle process of elemental separation postulated by Navon and Stolper (1987), matrix and metasomatizing melt or fluid contain common ions (Fig. 1b); also, the patterns created by preferential fractionation of LREE into liquid during percolation must be recorded in matrix. According to Navon and Stolper (1987) the evolving composition of percolating melts appears in matrix at the top of the column (implicitly a fixed distance from the source); transient incompatible-element fractionation is recorded early in the process. Fractionated melt compositions are progressively replaced by ones that tend toward and ultimately achieve equilibrium with the original melt composition (Fig. 1a, 1b; Navon and Stolper, 1987, their Fig. 4). The actual compositions produced in liquid and recorded by the matrix may be nearly any shape; the critical controls are the original compositions and relative volumes of matrix and melt, the actual partition coefficients at the conditions of reaction, and the actual process of exchange.

Important questions that are unanswered by Navon and Stolper (1987) include: What region of the mantle constitutes the top of a reacting column? Why does the migrating melt react in this region if the matrix is the same as that within the column? Why does the matrix pattern so accurately reproduce that in the melt if K_d values remain constant? What is the likely proportion of melt relative to matrix that can percolate far enough to produce the transient fractionation patterns?

Lherz massif, France

Structural, petrologic, and geochemical features. Models of mantle reactions were formulated by Bodinier et al. (1990) from systematic sampling of a harzburgite talus boulder. The boulder (Fig. 2a) contains an amphibole pyroxenite dike (vein, cf. Bodinier et al., 1990), and two branching "amphibole veinlets" occur within ~25 cm of the dike contact. Harzburgite within 25 cm of the dike contains amphibole, and the remainder lacks amphibole. The amphibole pyroxenite dike is garnet-bearing, and peridotite across the entire sampling traverse contains irregularly distributed secondary spinel and minor apatite (Woodland et al., 1992).

Mineral compositions are variable in the zone of amphibole-bearing harzburgite; interstitial amphibole and minor phlogopite are relatively poorer in Ti, Al, and Fe, compared with the same minerals in the dike and veinlets. The compositions of clinopyroxene, orthopyroxene, olivine, and spinel close to amphibole veinlets show reaction gradients of major and minor elements (Bodinier et al., 1990, their Fig. 3) such as are observed at contacts between peridotite and mafic dikes in composite xenoliths (Irving, 1980; Wilshire et al., 1980; Kempton et al., 1984; Wilshire et al., 1988).

REE_{cn} patterns of whole rock samples within ~15 cm of the dike have relatively unfractionated shapes that closely resemble that of the dike, but at slightly lower $LREE/HREE_{cn}$ (Fig. 2c); however, even assuming that the Yb content of sample 12 is 0.104 ppm (not 0.014 as tabulated) the Ce/Yb_{cn}, Sm/Yb_{cn}, and Tb/Yb_{cn} ratios for samples at 3 and 12 cm are 1.5–2 times those of other samples in the amphibole-bearing zone (Fig. 2a). Beginning in the amphibole-bearing harzburgite at ~16 cm from the dike contact and extending through the amphibole-free harzburgite, whole rock samples have U-shaped REE patterns, and samples 18, 21, 22 all have values comparable with those of samples 3 and 12 (Fig. 2a, 2c). Samples >22 cm from the dike contact, in the amphibole-free zone, have REE_{cn} patterns with negative slopes and progressively higher Ce/Yb_{cn} values (Fig. 2a, 2d). The relative LREE-enrichments reach a maximum of 16.4 times chondrite at 49 cm and then decrease to less than eight times chondrite in the sample at 65 cm (Fig. 2a). The progression of LREE enrichment in the Lherz boulder shows the sort of effect postulated by Navon and Stolper (1987), and thus provides a test of that particular hypothesis of chromatographic fractionation in the mantle.

Lherz models. Bodinier et al. (1990) explained the compositional variations of the Lherz sample as related to a single metasomatic event. They proposed that a melt infiltration process deposited amphibole in harzburgite between the dike contact and samples at ~21 cm without marked enrichment fronts of incompatible-elements in the peridotite. They ascribed REE_{cn} patterns in amphibole-free harzburgite to chromatographic fractionation of melt having the same composition as the liquid that produced the modal metasomatism. The fractionated melt was buffered by passage through the amphibole harzburgite. Bodinier et al. (1990) questioned whether the metasomatizing agents of the two processes are from the same or different sources but concluded that they represent evolution of infiltrating melt derived from the same source (the dike). Vasseur et al. (1991) also indicated that the two processes represent "a variation from bulk REE enrichment close to the vein, to selective LREE enrichment further away from it," thus ascribing both effects to the same metasomatic source.

Modal metasomatism: Diffusion controlled model. The diffusion-controlled model of modal metasomatism of the Lherz boulder proposed by Bodinier et al. (1990) requires infiltration of parent magma from the amphibole pyroxenite dike into adjacent wall rock (Fig. 3). The composition of infiltrating melt (Fig. 2b) was constructed by Bodinier et al. (1987) as a model of magmas (likened to alkali basalt) considered to be parental to the amphibole

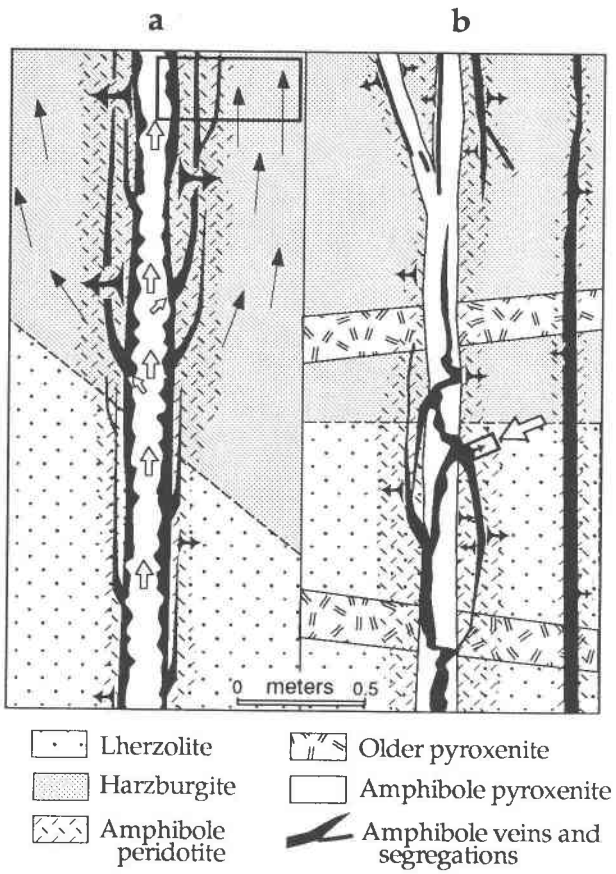

Fig. 3. Diagrams illustrating differing assumptions of metasomatic models. (**a**) Lherz model of Bodinier et al. (1990, adapted from their Fig. 9). Thick open arrows indicate supposed direction of dike intrusion, and thick black arrows show movement of melt diffusing into wall rock peridotite from dikes. Thin black arrows show percolation direction of alkali basalt melt inferred to have produced cryptic metasomatism. Rectangle indicates area of the sampled boulder. (**b**) Dish Hill model of Nielson et al. (1993; see Fig. 5). Relations of peridotite wall rocks, older pyroxenite dikes, amphibole pyroxenite dikes, and related amphibole veins, based on field relations observed at Lherz (Fig. 4) and on relations in xenoliths. Open arrow pointing at box indicates one of many possible positions of the Dish Hill xenolith in the original context.

pyroxenite dikes at Lherz and Freychinède. The calculated REE contents of such parent magmas are based on a liquid in equilibrium with amphibole in the dike. Amphibole veinlets are considered to provide evidence of melt circulation through the wall rock, and the crystallization of amphibole is thought to result from "interaction of the alkali basalt and peridotite" (Bodinier et al., 1990), consuming mainly clinopyroxene and spinel from wall rock. Steep compositional gradients of major elements adjacent to contacts with the dike are interpreted as resulting from diffusion between magma in the dike conduit and the infiltrating melt.

Our field and petrographic observations at Lherz (Wilshire et al., 1988; Nielson et al., in preparation) do not support this reaction sequence of magmas with peridotite. The relations between amphibole pyroxenite dikes and amphibole veinlets strongly indicate that amphibole was the last major phase to crystallize from amphibole pyroxenite dikes and that many amphibole veinlets originated as late segregations that emerged from the dikes. Intrusions that formed amphibole pyroxenite dikes first reacted with peridotite to form thin borders of amphibole-free pyroxenite, contrary to the inference of Bodinier et al. (1990; Fig. 3a). Within the reaction borders, fractional crystallization appears to have concentrated the amphibole component into late crystallizing liquids, where it forms segregations (Figs. 3b, 4a, 4b) and, in some dikes, interstitial poikilitic grains.

Some exposures at Lherz show that an amphibole-rich residual liquid infiltrated peridotite wall rock for a few centimeters, creating zones of amphibole peridotite such as those described by Bodinier et al. (1990) (Fig. 4a), but many other outcrops or talus boulders show dikes with internal amphibole segregations or dikes with irregular amphibole-rich zones that meander from axis to margin. Locally, residual liquid was injected into fractures within or external to the dike in which the liquid evolved (Fig. 4a, 4b). The residual melts injected into wall rock also reacted with and infiltrated the peridotite (Wilshire, 1984, 1987; Wilshire et al., 1988; Mukasa et al., 1991; Nielson et al., 1993, in preparation). Similar relations are observed in xenoliths (Fig. 4c).

The unmetasomatized composition of the Lherz boulder is not known (the model composition is highly LREE-depleted) (Bodinier et al., 1990, their Fig. 12b), but whole-rock REE patterns of amphibole peridotite in the zone of diffusion metasomatism reflect those of the dike (Bodinier et al., 1990, their Fig. 6). The REE compositions could be explained by the mixing of depleted peridotite and melt of the dike composition; therefore, we see no compelling reason for construction of a parent magma composition to represent the infiltrating liquid. We contend that actual compositions of the amphibole pyroxenite dike in the Lherz boulder or residual liquids from crystallization of the dike, represented by amphibole segregations that intruded peridotite as smaller veinlets (Fig. 3b; cf. Nielson et al., 1993), are plausible sources and compositions of the metasomatic melts.

Data presented by Bodinier et al. (1990) further suggested that the Lherz boulder contains more than one source of metasomatizing melt; for example, mineral compositions show gradients in the vicinity of the veinlets (Bodinier et al., 1990, their Fig. 3). According to the model calculations (Bodinier et al., 1990, their Fig. 11), a sample 1 cm from the amphibole pyroxenite dike should have the highest overall REE_{cn} and $LREE_{cn}$, and values should decline systematically with progressively greater distance from the contact. To the contrary, the sample at 12 cm from the pyroxenite dike contact (Fig. 2a, 2c) has the highest REE_{cn}, $LREE_{cn}$, and Ce/Yb_{cn} values reported

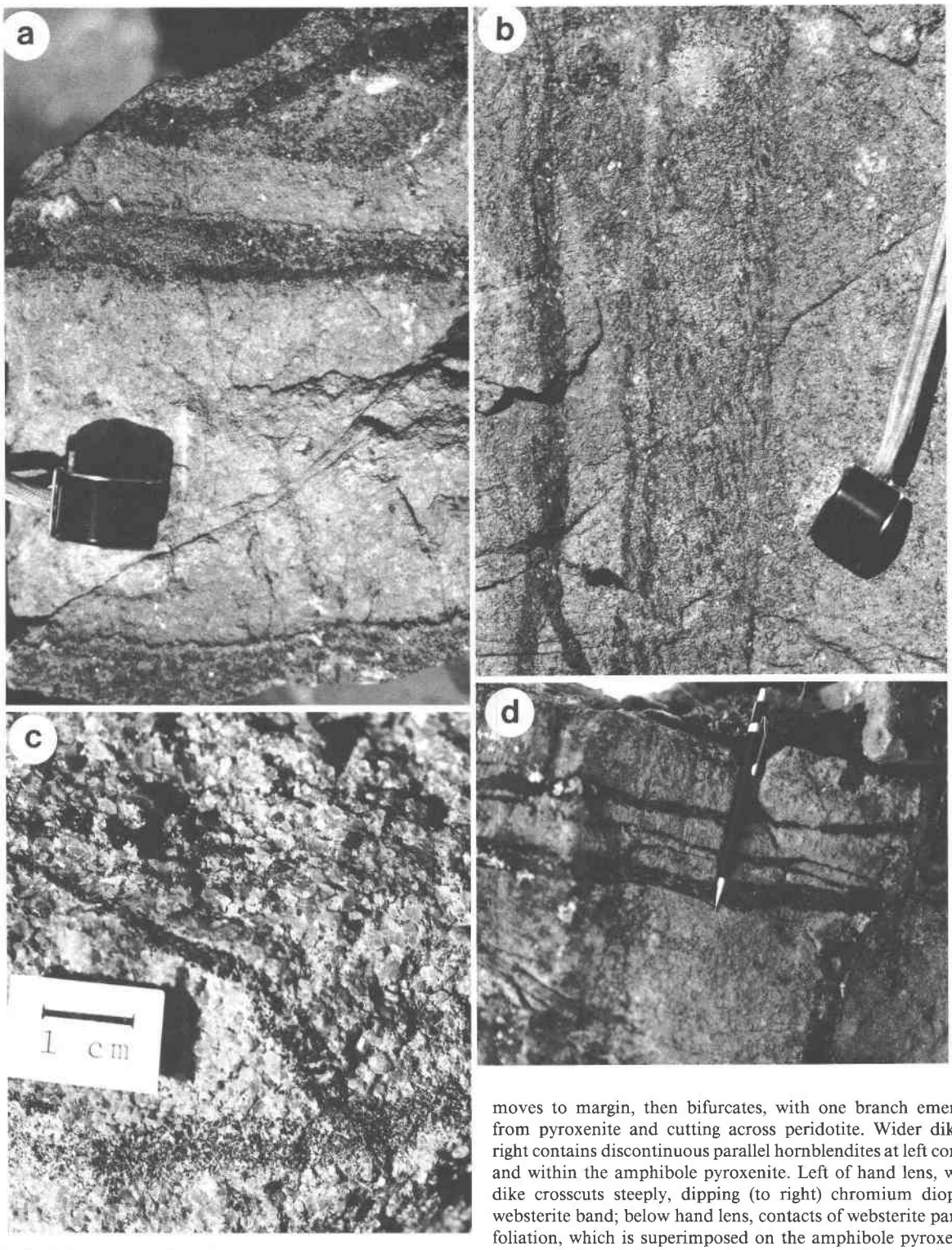

Fig. 4. Photographs of relations between dike and wall-rock peridotite. (**a**) Amphibole pyroxenite dikes in peridotite, Lherz massif. Some of the amphibole pyroxenite dikes have thin amphibole-free pyroxenite reaction rims and irregularly distributed amphibole-rich segregations (dark bands). (**b**) Amphibole pyroxenite dikes, Lherz massif. Left side of photo, from top to bottom, amphibole-rich band (dark) originates in amphibole pyroxenite, moves to margin, then bifurcates, with one branch emerging from pyroxenite and cutting across peridotite. Wider dike to right contains discontinuous parallel hornblendites at left contact and within the amphibole pyroxenite. Left of hand lens, wider dike crosscuts steeply, dipping (to right) chromium diopside websterite band; below hand lens, contacts of websterite parallel foliation, which is superimposed on the amphibole pyroxenite. These relations indicate that the amphibole grains in peridotite are not formed by reaction between dike parent magma and peridotite. (**c**) Xenolith from San Carlos, Arizona, showing thin amphibole-rich veinlet emerging from parent amphibole pyroxenite dike (nearly horizontal, lower part of photo) and cutting peridotite. (**d**) Photograph of anastomozing hornblendites, showing opposing directions of branching. Lherz massif.

from the zone of amphibole-bearing harzburgite (Ce/Yb_{cn} 1.6; the value for sample 1 is 0.90; Bodinier et al., 1990). Samples 3 and 18 also do not fit the model; sample 3 has the highest LREE of any sample in the amphibole-bearing zone, and sample 18 has a value of Ce/Yb_{cn} identical to that of sample 3. We conclude, therefore, that multiple sources of metasomatic fluids are present in the boulder, and their presence probably determined the width of the amphibole-bearing zone.

Cryptic metasomatism: Percolation controlled model. The cryptic metasomatic model devised by Bodinier et al. (1990) to explain REE patterns in the amphibole-free peridotite zone of the Lherz boulder "involves the evolution of a magma buffered by an amphibole peridotite mineralogy, probably as a result of interaction between the infiltrated alkali basalt and the peridotite matrix in the modally metasomatized wall rocks." LREE "escape the buffering effect, because of their strongly incompatible character" and thus become enriched in the melt during percolation. Contrary to Navon and Stolper (1987), the melts do not begin to fractionate until they percolate >1 m from the source (Bodinier et al., 1990; their Fig. 12b). This distance seems to establish an upper dimension for the width of reaction zones at dike contacts, which are ascribed to diffusion-controlled reactions (see above). Taken together, these statements imply that the melts were buffered by the contact zones.

Various aspects of this model are inconsistent with experimental data and other considerations. The upper temperature limit of amphibole stability (pargasite and kaersutite ~1050–1110 °C; Millhollen et al., 1974; Merrill and Wyllie, 1975) at the emplacement pressure of 10–15 kbar estimated by Bodinier et al. (1990) is too low to permit crystallization of amphibole at the near-solidus peridotite temperatures needed to propagate infiltration by this scheme. Therefore, the initial formation of an amphibole peridotite modal metasomatic zone needed to buffer additional infiltrating melts from the dike appears unlikely.

Other problems with the model are exemplified in Figure 12 of Bodinier et al. (1990), which shows the model anomalies plotted against the length of the percolation path for a range of values dependent on melt fraction, elapsed time, grain size ratios, and diffusive coefficients. The chromatographic calculation produces compositional changes that resemble results of Navon and Stolper (1987, their Fig. 4), but the sequence of reactions is reversed (Bodinier et al., 1990, their Figs. 12b and 13). The calculations of Navon and Stolper (1987) showed progressive compositional changes over time in a matrix that is located a fixed distance from the source of melt (top of the column), and this matrix region progresses toward equilibrium with the original melt. In contrast, Bodinier et al. (1990) showed progressive changes in the degree of REE fractionation, which are recorded in peridotite volumes at progressively more distant locations from the source of melt. High Ce/Yb_{cn} values occur because the melts retain LREE and are depleted, first in HREE and then in middle REE, at progressively larger distances along the percolation path. After 50 m of percolation the HREE contents merge into those of the assumed premetasomatic harzburgite (the actual composition is unknown). When the effect of melt volumes is accounted for, the degree of middle REE depletion increases for greater percolation distances. Ce/Yb_{cn} values comparable with those of sample 49 are produced after percolation of about 100 m.

The time factors of this model are very large. For the percolating melt, Bodinier et al. (1990) defined a parameter t_c as "the time it takes for the melt to pass throughout the distance of percolation." Assuming reasonable rates of percolation (u), they state that no Ce/Yb_{cn} anomaly is calculated for distances (z) that require <100 yr of percolation ($z = t_c u$) (p. 619). Between 5000 and 25000 yr are required to develop the small degrees of fractionation (Ce/Yb_{cn} between 8 and 16) that occur over distances of <1 km, according to the calculation. Refinements to the model by Vasseur et al. (1991) show evolution of the patterns extending over 50–2000 yr, much smaller percolation distances (3 m), and lower degrees of HREE depletion.

The expectation that melt can be supplied through narrow mantle conduits for periods longer than a few weeks is not supported either by considerations of duration and periodicity of mantle melt extraction events (Nicolas, 1989), or of heat loss (Spera, 1987). Moreover, at the high temperatures required to propagate the infiltration, melt in conduits as wide as 1 m might disperse into wall rocks in 100 yr (Watson, 1982). Since the Lherz massif contains a variety of older pyroxenite dikes (Figs. 3b, 4a), it seems evident that ambient temperatures were well below the peridotite solidus when the amphibole pyroxenites were emplaced.

To prevent small veinlets and infiltrating melt from rapidly freezing, the younger dikes would have to heat adjacent peridotite over the distances of measured anomalies and postulated scales of infiltration, to temperatures at or above the liquidus of the supposed parental alkali basalt (about 1275–1300 °C; e.g., Green and Ringwood, 1967; Takahashi, 1980). Liquidus temperatures of alkali basalt are slightly above the dry peridotite solidus and well above the wet peridotite solidus (Wyllie, 1979). Evidence of partial melting in the peridotites and especially in older pyroxenites crosscut by amphibole pyroxenite should be found if the hypothesis is correct. At lower temperatures, interstitial crystallization of liquidus and near-liquidus phases, or reaction products of the parent magma, ought to be evident in the amphibole-free harzburgite, but only green spinel and apatite, products of residual liquids, have been identified so far (Woodland et al., 1992).

In Figure 3, the model relations assumed by Bodinier et al. (1990) are compared with observed field relations among amphibole pyroxenite, derivative hornblendites, older dikes, and peridotite at Lherz, or reconstructed from xenoliths. The model suggests that the direction of veinlet

branching indicates the upward direction of infiltration for intrusions and melts in the mantle, if the infiltration was driven by melt buoyancy, as seems implied. Figure 3b schematically illustrates that dike branching may show opposing directions in a single outcrop, an observation documented in Figure 4d; therefore, the direction of branching is not a criterion for the absolute direction of magma movement in the plane of a tabular intrusion.

Xenolith from Dish Hill, California

Structural, petrologic, and geochemical features. Models of a mantle process resembling those in ion exchange columns for purifying liquids, such as H_2O softeners (Fig. 1c; Fletcher and Hofmann, 1974), were developed using data from a well-characterized amphibole-bearing spinel lherzolite xenolith from Dish Hill, California. The lherzolite xenolith is 17 cm long and has a thin (1 cm or thinner) hornblendite selvage (dike remnant) at one end (Wilshire et al., 1980, 1988; Nielson and Noller, 1987; Nielson et al., 1993; McGuire et al., 1991). Progressive changes in modal abundance and major-minor element composition of the interstitial amphibole grains and maps of fluid and solid inclusion abundances (Noller, 1986) show that interstitial amphibole grains and the inclusions are secondary and related to the selvage.

Steep compositional gradients of magmaphile major, minor, and trace elements, including LREE and some high field-strength elements (HFSE) such as Ta, formed in the rock a few centimeters from the contact between the hornblendite selvage and lherzolite. Within the most altered zone, HREE and some other compatible elements also are enriched, but to a lesser extent than elements that are commonly considered incompatible. Isotopic compositions also vary with respect to the contact (Fig. 5), such that the narrow (1.5–2 cm wide) contact zone of peridotite is close to isotopic equilibrium with the selvage (Nielson et al., 1993). Enrichment fronts of the various elements (Nielson et al., 1993, their Fig. 10) are slightly separated in peridotite within 4 cm of the dike selvage. These compositional variations are mostly due to reaction between clinopyroxene grains of the host rock and metasomatic melt from the dike, and wall rock relations accord more with the model of Bodinier et al. (1990) than the chromatographic fractionation scheme of Navon and Stolper (1987).

Dish Hill xenolith model. The reaction gradients in the Dish Hill xenolith can be modeled fairly well by simple finite-plate calculations (Fig. 6; Helferrich, 1962; Farmer and DePaolo, 1987), using end-member compositions in the sample. Amphibole in the selvage was used for the model liquid and refractory peridotite farthest from the selvage was presumed close to the unreacted composition of peridotite. The calculations employed by Nielson et al. (1993) are a simplification of Navon and Stolper's approach and agree with the concept that mantle reactions may be modeled by chromatographic processes. In contrast to the hypothesis of Navon and Stolper (1987), magmaphile elements in the Dish Hill sample including Rb,

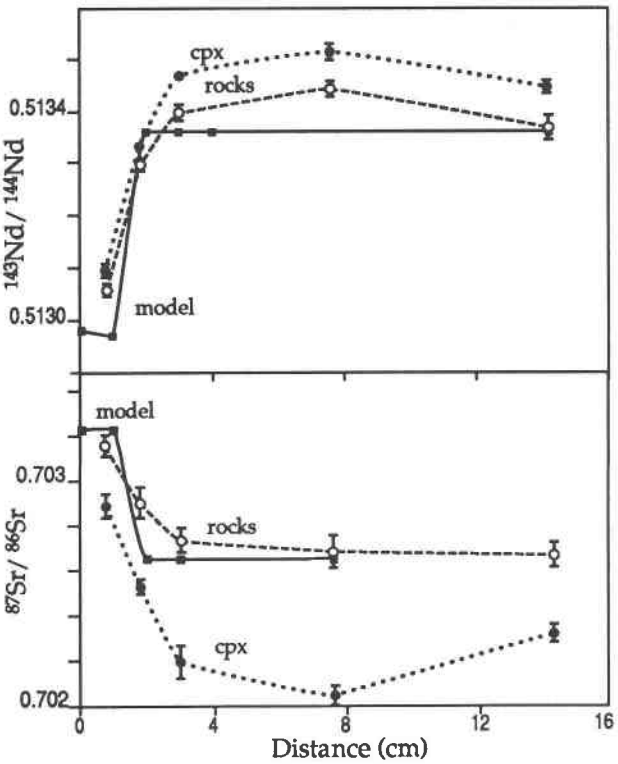

Fig. 5. A model of metasomatism for Dish Hill, CA xenolith Ba-2-1 (Nielson et al., 1993) based on reaction fronts of Nd- and Sr-isotopic ratios in lherzolite near contact with amphibole selvage (at 0). Data from five subsamples, from next to the contact to a distance of about 17 cm (rock compositions are shown by dashes and open circle symbols, clinopyroxenes by dotted lines, solid circles). Calculation of rock compositional variations (after Farmer and DePaolo, 1987) used mineral compositions and best-fit partition coefficients and assumed that the composition of infiltrating melt was that of dike. Concentration profiles calculated with a pure infiltration model (solid lines) neglected the effect of diffusion but are remarkably close to the position, shape, and compositional values of actual reaction fronts.

Ba, LREE, H_2O, and CO_2 (normally considered incompatible relative to peridotite) are enriched in peridotite close to the metasomatic source, as are compatible constituents of the melt. A small level of LREE enrichment is also seen in the peridotite subsample between 2 and 3 cm from the dike, and a slight U-shape is developed in that pattern. Therefore, although impoverished in LREE (as hypothesized by Bodinier et al., 1990) liquid continued to deposit LREE in the depleted peridotite as it moved farther from the contact zone. The decreased ratio of $LREE/HREE_{cn}$ in this reacted liquid is reflected in the decreased ratios recorded in the matrix at larger distances from the dike (Nielson et al., 1993, their Fig. 4). Therefore, the liquid became impoverished in incompatible elements with distance of percolation away from the dike contact zone, contrary to the assumptions of all percolative models (Navon and Stolper, 1987; Bodinier et al., 1990; and Harte et al., 1993).

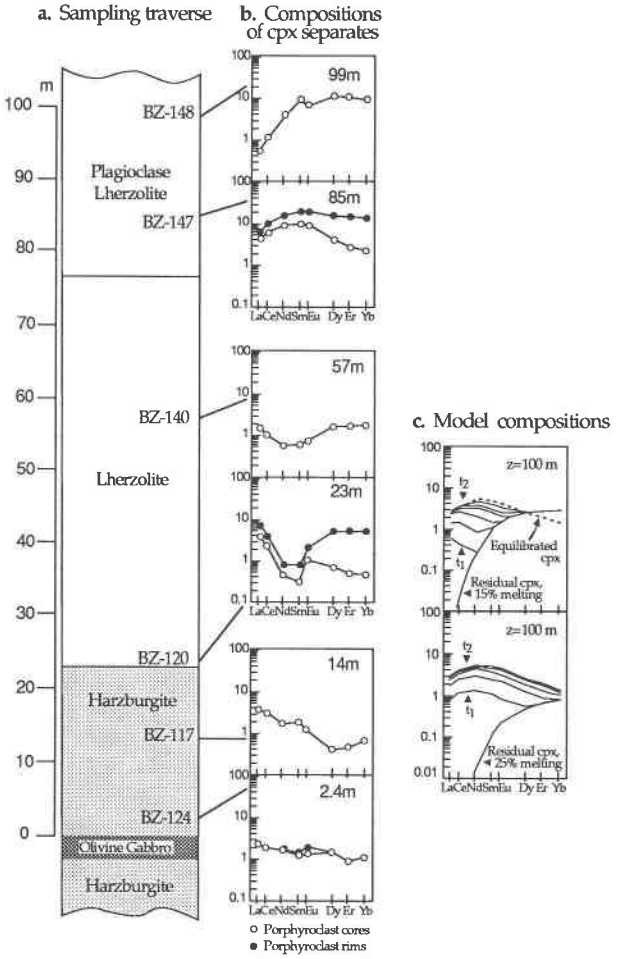

Fig. 6. Rock types and REE_{cn} variations in clinopyroxenes of the Horoman massif, compared with percolation models (combined Figs. 3 and 4 of Takazawa et al., 1992). Figs. rearranged for direct comparison of rock types, traverse distance, and sample REE_{cn} variations. (a) Rock type of sample, and distance on traverse, anchored by olivine gabbro (composition not given). Numbers are those samples given by Takazawa et al. (1992). (b) REE_{cn} compositions related to traverse position of samples. All compositional plots are at the same scale; labels of ordinate scale are removed for ease of reading—all are ratios of sample to chondrite. (c) Models of REE_{cn} patterns produced by interaction of peridotite varieties and melts from 15 and 25% melting, at 100-m percolation distance; models for 1 km were omitted because they are much less successful in matching patterns of the samples. The model plots have been changed to the same scale as all the sample plots.

REE patterns of the dike and metasomatized peridotite in the Dish Hill xenolith are similar to those of the Lherz boulder. The 1.5 cm of wall rock closest to the contact in the Dish Hill sample can be successfully modeled by simple mixing of end-member dike with unreacted peridotite (Budahn, 1991; Nielson et al., 1993). Convergence of Nd-isotopic values in rocks and clinopyroxenes (Fig. 5) shows that exchange of isotopic species between melt and clinopyroxenes can account for the metasomatic whole-rock composition, without crystallization interstitial amphiboles. In contrast, crystallization of new minerals (amphibole and solid inclusions) must account for higher Sr-isotopic compositions in the reacted lherzolite (cf. Nielson et al., 1993). A model of the reaction based on Isocon calculations of Grant (1986) suggest that equilibrium between the melt and depleted wall-rock peridotite may have required interaction between equivalent volumes of LREE-enriched liquid and rock in the 1.5-cm-thick contact zone (Nielson et al., 1993). The data suggest short time factors for these interactions.

Horoman massif, Japan

Structural, petrologic, and geochemical features. The Horoman massif crops out in an area of about 800 km^2. The rocks are well exposed along drainages, but substantial differences between maps of the complex (Niida, 1974; Obata and Nagahara, 1987; Takahashi, 1991; Takazawa et al., 1992) suggest that intervening areas are poorly exposed. The massif consists mostly of alternating bands of plagioclase lherzolite, lherzolite, and harzburgite that vary from a few meters to several hundred meters in thickness. Within the peridotite are gabbro dikes and phlogopite-rich veins (Takahashi, 1991; Takazawa et al., 1992). All peridotite variants (including dunite) have porphyroclastic and locally mylonitic textures. Zones of plagioclase-free lherzolite separate bands of plagioclase lherzolite and harzburgite, and parallel layers of dunite as much as 15 m thick occur locally in the harzburgite (Takahashi, 1992; Takazawa et al., 1992).

Magmaphile minor and trace elements (bulk peridotite-melt coefficients >1: Cr, Mn, Fe, Co, Ni, and Zn) show little variation between lherzolite varieties and harzburgite (Frey et al., 1991). Larger variations are shown by Ti, Sc, V, and Ga; plagioclase lherzolite has the highest and harzburgites have the lowest contents of these elements. Most whole rocks and clinopyroxenes show congruent REE patterns that are depleted in $LREE_{cn}$ and have relatively flat patterns for all middle and HREE. Exceptions are two harzburgite samples with relatively flat whole-rock patterns and clinopyroxenes enriched in $LREE_{cn}$ (Frey et al., 1991). Takazawa et al. (1992) reported variations of REE in clinopyroxene from a sampling traverse across adjacent layers of the main peridotite series, located by reference to a gabbro band (Fig. 5). The data show a variety of REE_{cn} patterns (Fig. 5b).

The bulk compositions of Horoman samples from a 100-m traverse (Fig. 6) all have values of La_{cn} and Ce_{cn} that are lower than chondrites. Three of the lherzolite samples (two plagioclase lherzolites) have chondrite-normalized values of 1–2 for the REE from Nd through Tb (Frey et al., 1991), and two harzburgite samples have La/Sm_{cn} values >1.0, although $LREE_{cn}$ contents are 0.1 (Frey et al., 1991). REE_{cn} patterns of clinopyroxene grains in these rocks are variously $LREE_{cn}$-depleted, slightly enriched (La/Sm_{cn} as much as 5), or have relatively high REE contents (Nd_{cn} as much as 13, Sm_{cn} of 16) and rel-

atively unfractionated REE_{cn} patterns. Some of the LREE-enriched patterns are U-shaped, so that $LREE/HREE_{cn}$ values do not reflect the level of LREE and middle REE enrichment. Frey et al. (1991) concluded that the presence of LREE enrichments is not consistent with melt extraction by which the main rock types formed and therefore postulated a later enrichment event.

Horoman model. The lherzolite and harzburgite bands are interpreted as restites from partial melting of plagioclase lherzolite protolith by Takahashi (1991, 1992), Frey et al. (1991), and Takazawa et al. (1992). Takahashi (1992) also interpreted the dunite zones interlayered with harzburgite, lherzolite, and plagioclase lherzolite to be a cumulate of melts related to the formation of restites. Arai and Takahashi (1989) interpreted phlogopite-rich veins and interstitial phlogopite as having crystallized from fluids released by evolving alkali basaltic magmas of unspecified origin. Takahashi (1992) further presented evidence that the gabbros formed as intrusions and that they metasomatized host dunite and harzburgite, locally depositing titanium pargasite, kaersutite, titanite, and ilmenite.

Because the REE patterns change abruptly in the rocks sampled, Takazawa et al. (1992) modeled the varied REE patterns of Horoman peridotite samples as being caused by chromatographic fractionation in a melt during percolation. The melt may or may not be related to a gabbro at one end of the transect. Following Navon and Stolper (1987) the model calculation assumes that changing fractionation patterns are recorded in matrix a fixed distance (100 m and 1 km) from the source (Takazawa et al., 1992). In modeling the progression of REE patterns in the peridotites, the authors postulated that harzburgite and lherzolites had different premetasomatic REE contents, due to the different degrees of partial melting (25 and 15%, respectively) that is thought to have created the rock types (Fig. 6c; only the 100-m model is shown). Residual clinopyroxene in harzburgite and lherzolite would have different metasomatic compositions after reaction with the same melt composition.

Taking these factors into account, the authors recognize that their calculations do not produce a simultaneous fit among pattern shape, level of enrichment, or percolation distance or time, if the percolation direction is parallel to the traverse (Takazawa et al., 1992). Close to the gabbro, patterns in harzburgite show a progressive enrichment in LREE with distance from the contact (samples at 2.4–14 m; Fig. 6), and these compositional changes correspond to those modeled for a sample 100 m from the source at progressively greater percolation times (sample at 2.4 m resembles the model of 25% melt residue metasomatized at t_1; sample at 14 m resembles the same residue metasomatized slightly later; Fig. 6c). Similarly, the lherzolite sample at 57 m fits the model of a residue from 15% melting, metasomatized at a time closer to t_2, and the pattern of a clinopyroxene core at 23 m represents the pattern for a stage between that time and t_1 (Fig. 6). However, the rim of that clinopyroxene has a deep U-shaped REE pattern with higher HREE than the core, which resembles the model for t_1.

According to the Navon and Stolper (1987) hypothesis, these fractionation patterns are transitory; patterns representing metasomatism by the earliest melts reaching the top of a mantle column should have been changed by interaction with melt aliquots that came later. In addition, the plagioclase lherzolite sample at 85 m should represent matrix that has reached equilibrium with the original melt composition; however, evidence of such an equilibrated peridotite column is not represented on the sampling traverse. Thus, a different trajectory of percolation is indicated, but the data do not support assessment of this possibility. The scheme of Bodinier et al. (1990), with some of the refinements of Vasseur et al. (1991), could explain variations between 99 and 57 m, but only if a nearby source could be identified.

The lack of congruence between data and the Horoman model, especially the HREE zonation in clinopyroxene grains, is of concern, and Takazawa et al. (1992) admitted that they need a more complex model. Also, more recent data for the gabbro layer in the 100-m section sampled indicate that it is not the source of the metasomatic fluids (F. A. Frey, personal communication). Thus, more data are needed to establish better constraints on the composition of the metasomatic agents, the directions and velocity of flow, and permeability.

Discussion

Mantle samples and process models

The models reviewed here share the assumption that reactions between mantle melts and peridotite are chromatographic processes, but they conflict in the choice of chromatographic processes that may emulate the reactions. Some models of elemental fractionation due to melt-peridotite interaction are based on the undocumented hypothesis that large melt volumes are transported through the upper mantle by pervasive, regional-scale percolation (cf. Navon and Stolper, 1987). These models contain additional assumptions that conflict with each other and with evidence from constrained studies of xenoliths and massifs.

The samples chosen for modeling are critical to establishing appropriate constraints. Models based on xenoliths cannot be tested unless composite samples (with evidence of their context) are used. This limitation should not be a problem for massifs, because sample contexts are observable. The ability to observe context makes the study of massifs particularly valuable, but it also implies major logistical commitments for adequate testing of hypotheses and models.

Data from composite samples can provide important observations relevant to the debate about mantle processes. Composite xenoliths contain all the rock types and contact relations that are observed in massifs. Xenoliths are relatively fresh, having been excavated from the mantle lithosphere in a matter of hours or days. In contrast,

peridotite massifs of the Pyrenees and Ivrea Zone have complex crustal emplacement and metamorphic histories (e.g., Quick and Sinigoi, 1992). Electron probe traverses across samples from contact zones between peridotite and pyroxenite or amphibole dikes of massifs show mineral compositional gradients like those in composite xenoliths (Hofmann et al., 1992; Nielson et al., in preparation), but many of these data are highly scattered due to partial reequilibration.

Model similarities and differences

The models of reactions in a composite xenolith from Dish Hill are based on observable compositions of unmetasomatized peridotite and metasomatic melt, which can be used to test the assumptions of percolative models and the hypothesis of Navon and Stolper (1987). The Dish Hill sample shows conclusively that chromatographic reactions can produce steep compositional gradients and abrupt reversals in REE_{cn} patterns (cf. Takazawa et al., 1992) over a distance of 17 cm. However, contrary to Navon and Stolper (1987), the most elevated $LREE_{cn}$ contents and fractionated patterns of $LREE_{cn}$ vs. $HREE_{cn}$ occur within 2 cm of the dike contact. In this zone, the originally depleted peridotite is in isotopic equilibrium with the dike composition and has a pattern of REE_{cn} that is similar to, but slightly lower than, that of the dike.

The Dish Hill data also raise questions about the application to mantle processes of the frontal method of chromatographic separation, which is the basis of Navon and Stolper's (1987) hypothesis. In the xenolith, LREE are deposited in the peridotite along with HREE, rather than being preferentially carried in the melt. Beyond the zone of greatest peridotite-melt reaction, the REE_{cn} pattern is slightly U-shaped. The cause of this fractionation is unclear, but it can be modeled as selective partitioning of middle REE by interstitial amphibole (Budahn, 1991). If the observation that REE are not preferentially retained in percolating liquid can be generally applied to mantle processes, the LREE probably do not fractionate during percolation.

Metasomatism of harzburgite is observed in the dike contact zone of the Lherz boulder, in accord with relations in the Dish Hill xenolith. Similar to Nielson et al. (1993), Bodinier et al. (1990) postulated that peridotite closest to the source of melt reflects equilibrium with the original melt composition. However, the Dish Hill model is consistent with a metasomatic melt composition that is very similar to the intrusive rock present in the sample. The REE patterns of amphibole peridotite in the Lherz boulder suggest that the metasomatic melt had a composition like that of the amphibole pyroxenite dike, instead of the theoretical parent magma (cf. Bodinier et al., 1990).

The Lherz models assume two metasomatic processes: the contact zone is metasomatized by a diffusion-controlled process, and, no matter what melt volume is discharged into the wall rock, the zone in equilibrium with melt apparently remains about 1 m wide. Beyond 1 m, the melt compositions are controlled by percolation; the fractionating melt is said to be buffered by the minerals in an amphibole peridotite, presumably in this contact zone. However, the melt percolates long distances beyond the diffusion-controlled zone (Bodinier et al., 1990, their Fig. 9), and HREE are progressively removed from the melt as the distance of percolation increases. Therefore, this part of the model does not accord with classical definitions of buffer systems, that compositions in a system of interacting liquid and solid remain relatively unchanged for components that are common to, and equilibrated with, both parts of the system (Krauskopf, 1967).

Preferred chromatographic model

On the basis of the Dish Hill data, the chromatographic process that most resembles observed and documented mantle reactions is similar to those of H_2O-purification columns (Fig. 1c; Helferrich, 1962; Hofmann, 1972; Fletcher and Hofmann, 1974). In a mantle region, relatively depleted peridotite reacts immediately with incompatible element-enriched melt, and a zone nearest the contact reaches equilibrium with a proportional volume of the melt. The liquid that moves beyond this zone has reduced potential to react further with the matrix (cf. Fig. 1c, left side). If additional volumes of the original melt composition enter the matrix, they first encounter peridotite in equilibrium with the melt composition and pass through unchanged; in this equilibrated zone the melt is buffered, sensu stricto.

Upon reaching the reaction boundary and encountering depleted peridotite, the buffered melt reacts as before, and the zone of equilibrated matrix moves farther away from the source (Fig. 1c, center); the reacted liquid has a reduced potential to exchange further, as before. In the mantle, this process is limited by the supply of melt because the abundance of depleted peridotite must be very much greater than volumes of enriched melts (Nielson et al., 1993). However, large melt volumes would produce increasingly thick zones of equilibrated peridotite, both by percolation and dike branching (Fig. 3b).

To preserve transitory patterns of fractionated REE in matrix, the hypothesis of Navon and Stolper (1987) requires passage of relatively small volumes of melt, because large volumes ultimately bring a matrix into equilibrium with the melt composition (Fig. 1a, 1b). In contrast, REE fractionation patterns calculated by Bodinier et al. (1990) are not transient for any melt volume. According to their model, matrix in equilibrium with melt is found only in the diffusion-controlled zone, within 1 m of the dike. Longer times of percolation (t_c) correspond to larger percolation distances and greater degrees of fractionation (Bodinier et al., 1990, their Fig. 13).

Tests of percolation scale in mantle metasomatism

Models based on regional, pervasive porous-medium flow in the mantle can be qualitatively evaluated in terms of the likelihood that the necessary conditions exist, but

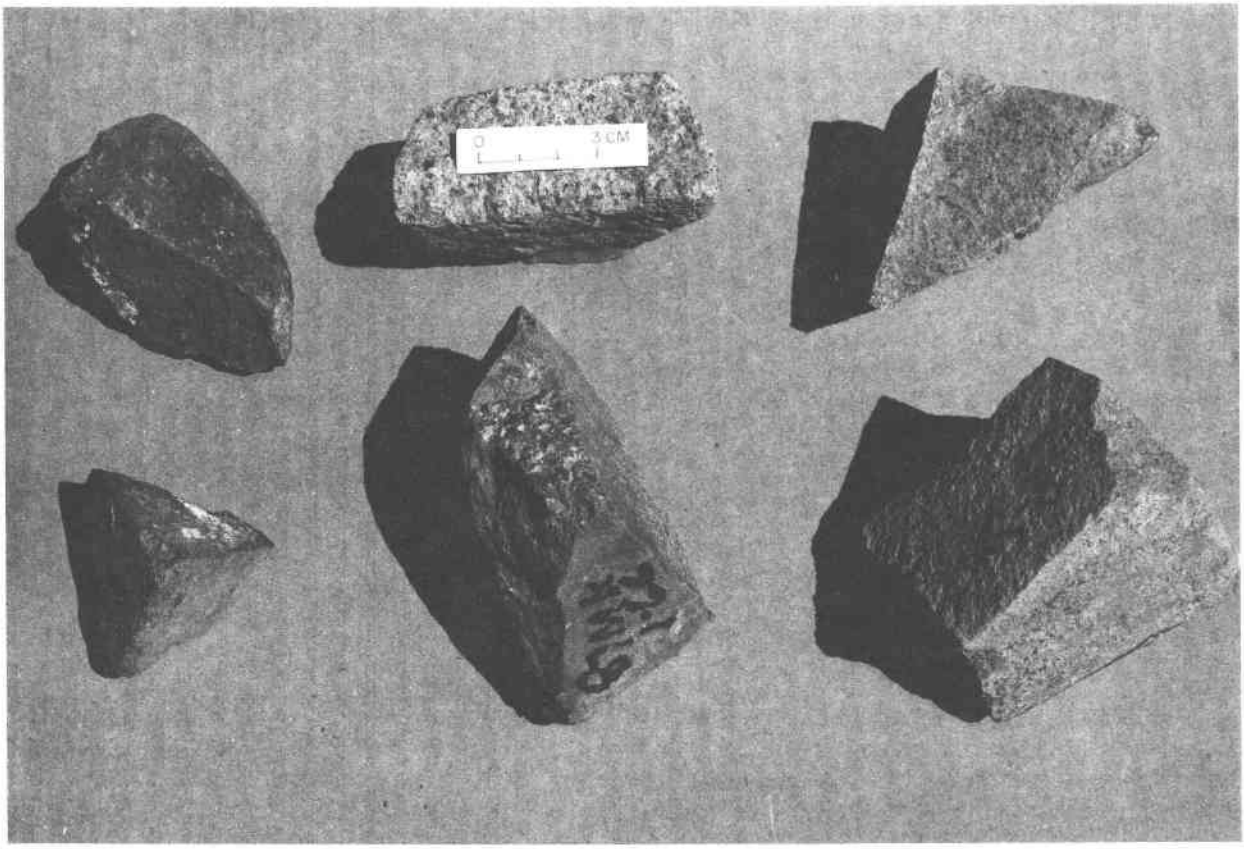

Fig. 7. Photograph showing the common faceted character of peridotite xenoliths in basalts. The facets are shown to be preentrainment joints (and shear fractures) by the common presence of intrusions along them that have compositions different from those of the host basalts (Wilshire and Kirby, 1989). From left to right, top: Victoria, Australia; Queensland, Australia; Massif Central, France; bottom: Cima, California; Hualalai, Hawaii; Jilin Province, China.

essentially they cannot be tested. In contrast, evidence of hydraulic fracturing is observed in xenolith samples worldwide, and the common observation of dikes representing multiple episodes of magmatism in mantle massifs points to the same conditions in their source regions. Particularly the xenolith samples, which do not share the crustal deformational history of massifs, show the evidence of intrusion in all their discernible magmatic history and hydraulic fracturing on centimeter scales in their most recent, preentrainment history (Fig. 7; Wilshire and Kirby, 1989). Where conditions in the source areas of mantle samples are favorable for hydraulic fracturing, porous flow probably could not successfully compete as a mechanism for fluid transport over substantial distances.

In our opinion, the evidence for metasomatism due to porous-medium flow on scales of tens of meters or kilometers has not yet been documented in massifs. Nevertheless, the trace element behavior in massifs showing large-scale (tens of meters) symmetrical lithologic variations remain to be explained. Current studies of the Lherz and Horoman massifs will add greatly to our knowledge, especially if hypotheses are adequately tested. From their recent study of the Lherz boulder, Woodland et al. (1992) concluded that throughout, "melt infiltrated non-pervasively, migrating along select grain boundaries, and interacting with the host to variable degrees." We note also that the refinements to the model of Bodinier et al. (1990) by Vasseur et al. (1991) deal with considerably reduced scales (<3 m) and times (<2000 yr), which shifts the boundary conditions of melt percolation closer to those observed in xenolith reactions and field relations. We therefore believe that the collection of systematic data from both massifs and xenoliths, focusing on all peridotite varieties and testing the assumptions about likely melt compositions, will ultimately bring convergence to chromatographic mantle models.

Geochemical studies of Horoman are at an early stage and thus amenable to tests of model assumptions, particularly because the field relations have been closely examined (Niida, 1974; Obata and Nagahara, 1987; Takahashi, 1991). In addition to sampling scale, the lack of fit between data from Horoman samples and the model could be tested by sampling for small-scale metasomatism due to localized melt conduits. For example, metasomatic agents might have been distributed through a complex of

now-healed fractures that allowed local infiltration. All current hypotheses for the origin of the main lithologic variants at Lanzo in the Ivrea Zone (Boudier and Nicolas, 1977; Boudier, 1978) and the Trinity massif in California (Quick, 1981), as well as at Horoman, propose an early depletion of the protolith by various degrees of partial melting. These hypotheses all require later healing of conduits that must have removed the partial melts; therefore, our working hypothesis is plausible. A more complex model may be needed for Horoman, as suggested by Takazawa et al. (1992), but it seems more appropriate to first test model assumptions where the data conflict, by analyzing finer scale samples. Test of percolation direction can be made by sampling on traverses that parallel the individual bands.

Conclusions

Mantle rocks provide limited and commonly ambiguous evidence for models of metasomatic processes, and the boundary conditions of those models conflict. However, evidence abounds in massifs and xenolith suites for mantle metasomatic processes by short-scale percolation in wall rocks close to single or multiple sources of melts. Most well-studied occurrences display multiple episodes of magmatism. In contrast, melt percolation on scales greater than several meters is still speculative.

Well-documented reactions between mantle peridotite and basaltic melts with enrichment fronts of incompatible elements, both in xenoliths (Nielson et al., 1993) and massifs (Bodinier et al., 1990; Woodland et al., 1992; Hofmann, et al., 1992), show that dike contact zones are most likely to reach equilibrium with the melt compositions, and that mantle metasomatism imprints the compositions of melts in conduits upon relatively depleted peridotite in these zones.

Studies of samples or sample suites that are carefully selected for well-defined contact relations and evidence of single-stage reactions are more likely to produce successful models of mantle processes than are large-scale studies of bodies with highly complex histories. We suggest that congruence among the models will come from such well-constrained studies. Refinements of one percolative model already trend toward smaller time frames and areal effects.

Acknowledgments

We are indebted to Darby Dyar, University of Oregon, Anne McGuire, University of Houston, Adolphe Nicolas, University of Montpellier, Joseph Arth, U.S. Geological Survey, and an anonymous reviewer for extremely helpful criticisms and corrections of our misconceptions. Additional clarifications were provided by correspondence with F.A. Frey, Massachusetts Institute of Technology, and J.L. Bodinier, University of Montpellier and discussions with Douglas Smith, University of Texas.

References cited

Anders, E., and Ebihara, M. (1982) Solar-system abundances of the elements. Geochimica et Cosmochimica Acta, 46, 2363–2380.

Arai, S., and Takahashi, N. (1989) Formation and compositional variation of phlogopites in the Horoman peridotite complex, Hokkaido, northern Japan: Implications for origin and fractionation of metasomatic fluids in the upper mantle. Contributions to Mineralogy and Petrology, 101, 165–175.

Bodinier, J.L., Fabriès, J., Lorand, J.P., Dostal, J., and Dupuy, C. (1987) Geochemistry of amphibole pyroxenite veins from the Lherz and Freychinède ultramafic bodies (Ariège, French Pyrenees). Bulletin de Minéralogie, 110, 345–358.

Bodinier, J.L., Vasseur, G., Vernières, J., Dupuy, C., and Fabriès, J. (1990) Mechanisms of mantle metasomatism: Geochemical evidence from the Lherz orogenic peridotite. Journal of Petrology, 31, 597–628.

Boudier, F. (1978) Structure and petrology of the Lanzo peridotite massif (Piedmont Alps). Geological Society of America Bulletin, 52, 39–56.

Boudier, F., and Nicolas, A. (1977) Structural controls on partial melting in the Lanzo peridotites. In H.J.B. Dick, Ed., Magma genesis, p. 63–78. Oregon Department of Geology and Mineral Industries, Bulletin 96, Portland, Oregon.

Budahn, J.R. (1991) An empirical equation to model rare earth element mineral-mineral partitioning: An application to mantle metasomatism. U.S. Geological Survey Open-File Report, OF 91-0596.

Bussod, G.Y., and Christie, J.M. (1991) Textural development and melt topology in spinel lherzolite experimentally deformed at hypersolidus conditions. Journal of Petrology, Special Lherzolites Issue, 17–39.

Daines, M.J., and Kohlstedt, D.L. (1993) A laboratory study of melt migration. Philosophical Transactions of the Royal Society of London, Series A, 342, 43–52.

Dawson, J.B., and Smith, J.V. (1992) Olivine-mica pyroxenite xenoliths from northern Tanzania: Metasomatic products of upper-mantle peridotite. Journal of Volcanology and Geothermal Research, 50, 131–142.

Eggler, D.H. (1987) Solubility of major and trace elements in mantle metasomatic fluids: Experimental constraints. In M.A. Menzies and C.J. Hawkesworth, Eds., Mantle metasomatism, p. 21–42. Academic, New York.

Eggler, D.H., and Holloway, J.R. (1977) Partial melting of peridotite in the presence of H_2O and CO_2: Principles and review. In H.J.B. Dick, Ed., Magma genesis, p. 15–36. State of Oregon Department of Geology and Mineral Resources Bulletin 96, Portland, Oregon.

Farmer, G.L., and DePaolo, D.J. (1987) Nd and Sr isotope study of hydrothermally altered granite at San Manuel, Arizona: Implications for element migration paths during the formation of porphyry copper ore deposits. Economic Geology, 82, 1142–1151.

Fletcher, R.C., and Hofmann, A.W. (1974) Simple models of diffusion and combined diffusion-infiltration metasomatism. In A.W. Hofmann, B.J. Giletti, H.S. Yoder, Jr., and R.A. Yund, Eds., Geochemical transport and kinetics. Carnegie Institution of Washington Publication, 634, 243–259.

Frey, F.A., Shimizu, N., Leinbach, A., Obata, M., and Takazawa, E. (1991) Compositional variations within the lower layered zone of the Horoman peridotite, Hokkaido, Japan: Constraints on models for melt-solid segregation. Journal of Petrology, Special Lherzolites Issue, 211–227.

Fujii, N., Osamura, K., and Takahashi, E. (1986) Effect of water saturation on the distribution of partial melt in the olivine-pyroxene-plagioclase system. Journal of Geophysical Research, 91, 9253–9259.

Grant, J.A. (1986) The isocon diagram: A simple solution to Gresens' equation for metasomatic alteration. Economic Geology, 81, 1976–1982.

Green, D.H., and Ringwood, A.E. (1967) The genesis of basaltic magmas. Contributions to Mineralogy and Petrology, 15, 103–190.

Harte, B. (1983) Mantle peridotites and processes: The kimberlite sample. In C.J. Hawkesworth and M.J. Norry, Eds., Continental basalts and mantle xenoliths, p. 46–91. Shiva, Cheshire, U.K.

Harte, B., Hunter, R.H., and Kinny, P.D. (1993) Melt geometry, movement and crystallization in relation to mantle dykes, veins and metasomatism. Philosophical Transactions of the Royal Society of London, Series A, 342, 1–21.

Helferrich, F. (1962) Ion exchange, 624 p. New York, McGraw-Hill.

Hofmann, A.W. (1972) Chromatographic theory of infiltration metasomatism and its application to feldspars. American Journal of Science, 272, 69–90.

Hofmann, A.W., Lu, M., Obermiller, W., Rivalenti, G., and Mazzucchelli, M. (1992) Contrasting styles of crustal contamination in Ivrea magma chambers and peridotites (abs.). In J.E. Quick and Silvano

Sinigoi, Eds., Ivrea-Verbano zone workshop, 1992, p. 10. U.S. Geological Survey Circular 1089.

Irving, A.J. (1980) Petrology and geochemistry of composite ultramafic xenoliths in alkalic basalts and implications for magmatic processes within the mantle. American Journal of Science, 280-A, 389–426.

Kelemen, P.B., Dick, H.J.B., and Quick, J.E. (1992) Formation of harzburgite by pervasive melt/rock reaction in the upper mantle. Nature, 358, 635–641.

Kempton, P.D., Menzies, M.A., and Dungan M.A. (1984) Petrography, petrology and geochemistry of xenoliths and megacrysts from the Geronimo volcanic field, southeastern Arizona. In J. Kornprobst, Ed., Kimberlites. II. The mantle and crust-mantle relationships, p. 71–83. Elsevier, New York.

Krauskopf, K.B. (1967) Introduction to geochemistry, 721 p. McGraw Hill, New York.

Lloyd, F.E, Nixon, P.H., Hornung, G., and Condliffe, E. (1987) Regional K-metasomatism in the mantle beneath the west branch of the East African Rift: Alkali clinopyroxenite xenoliths in highly potassic magmas. In P.H. Nixon, Ed., Mantle xenoliths, p. 641–659. Wiley, New York.

McGuire, A.V., Dyar, M.D., and Nielson, J.E. (1991) Metasomatic oxidation of upper mantle peridotite. Contributions to Mineralogy and Petrology, 109, 252–264.

McKenzie, D.P. (1984) The generation and compaction of partially molten rock. Journal of Petrology, 25, 713–765.

Merrill, R.B., and Wyllie, P.J. (1975) Kaersutite and kaersutite eclogite from Kakanui, New Zealand: Water-excess and water-deficient melting to 30 kilobars. Geological Society of America Bulletin, 86, 555–570.

Millhollen, G.L., Irving, A.J., and Wyllie, P.J. (1974) Melting interval of peridotite with 5.7 percent water to 30 kilobars. Journal of Geology, 82, 575–587.

Mukasa, S.B., Wilshire, H.G., Nielson, J.E., and Shervais, J.W. (1991) Intrinsic Nd, Pb and Sr isotopic heterogeneities exhibited by the Lherz alpine peridotite massif, French Pyrenees. Journal of Petrology, Special Lherzolites Issue, 117–134.

Navon, O., and Stolper, E. (1987) Geochemical consequences of melt percolation: The upper mantle as a chromatographic column. Journal of Geology, 95, 285–307.

Nicolas, A. (1986) A melt extraction model based on structural studies in mantle peridotites. Journal of Petrology, 27, 999–1022.

——— (1989) Structures of ophiolites and dynamics of oceanic lithosphere. Kluwer Academic, Boston, Massachusetts.

——— (1990) Melt extraction from mantle peridotites: Hydrofracturing and porous flow, with consequences for oceanic ridge activity. In M.P. Ryan, Ed., Magma transport and storage, p. 159–173. Wiley, New York.

Nielson, J.E., and Noller, J.S. (1987) Processes of mantle metasomatism. In E.M. Morris and J.D. Pasteris, Eds., Mantle metasomatism and alkaline magmatism. Geological Society of America Special Paper, 215, 61–76.

Nielson, J.E., Budahn, J.R., Unruh, D., and Wilshire, H.G. (1993) Actualistic models of mantle metasomatism. Geochimica et Cosmochimica Acta, 57, 105–121.

Niida, K. (1974) Structure of the Horoman ultramafic massif of the Hidaka metamorphic belt in Hokkaido, Japan. Geological Society of Japan, 80, 31–44.

Noller, J.S. (1986) Solid and fluid inclusions in mantle xenoliths: An analytical dilemma? Geology, 14, 437–440.

Obata, M., and Nagahara, N. (1987) Layering of alpine-type peridotite and the segregation of partial melt in the upper mantle. Journal of Geophysical Research, 92, 3467–3474.

O'Reilly, S.Y., Griffin, W.L., and Ryan, C.G. (1991) Residence of trace elements in metasomatized spinel lherzolite xenoliths: A proton-microprobe study. Contributions to Mineralogy and Petrology, 109, 98–113.

Phipps-Morgan, J. (1987) Melt segregation beneath mid-ocean spreading centers. Geophysical Research Letters, 14, 1238–1241.

Quick, J.E. (1981) The origin and significance of large, tabular, dunite bodies in the Trinity Peridotite, northern California. Contributions to Mineralogy and Petrology, 78, 413–422.

Quick, J.E., and Sinigoi, S., Eds. (1992) Ivrea-Verbano zone workshop, 1992. U.S. Geological Survey Circular 1089.

Rabinowicz, M., Ceuleneer, G., and Nicolas, A. (1987) Melt segregation and flow in mantle diapirs below spreading centers: Evidence from the Oman ophiolite. Journal of Geophysical Research, 92, 3475–3486.

Ribe, N.M. (1985) The generation and composition of partial melts in the earth's mantle. Earth and Planetary Science Letters, 73, 361–376.

Riley, G.N., Jr., and Kohlstedt, D.L. (1990) An experimental study of melt migration in an olivine melt system. In M.P. Ryan, Ed., Magma transport and storage, p. 77–86. Wiley, New York.

Ritchie, A.S. (1964) Chromatography in geology, 185 p. Elsevier, New York.

Ryan, M.P. (1988) The mechanics and three-dimensional internal structure of active magmatic systems: Kilauea volcano, Hawaii. Journal of Geophysical Research, 93, 4213–4248.

Samuelson, O. (1953) Ion exchanges in analytical chemistry, 291 p. Wiley, New York.

Shaw, H.R. (1980) The fracture mechanisms of magma transport from the mantle to the surface. In R.B. Hargraves, Ed., Physics of magmatic processes, p. 201–264. Princeton University Press, Princeton, New Jersey.

Sleep, N.H. (1988) Tapping of melt by veins and dikes. Journal of Geophysical Research, 93, 10255–10272.

Smith, D., Griffin, W.L., Ryan, C.G., and Sie, S.H. (1991) Trace-element zonation in garnets from The Thumb: Heating and melt infiltration below the Colorado Plateau. Contributions to Mineralogy and Petrology, 107, 60–79.

Smith, D., Griffin, W.L., and Ryan, C.G. (1993) Compositional evolution of high-temperature sheared lherzolite PHN 1611. Geochimica et Cosmochimica Acta, 57, 605–613.

Spera, F.J. (1987) Dynamics of translithospheric migration of metasomatic fluid and alkaline magma. In M.A. Menzies and C.J. Hawkesworth, Eds., Mantle metasomatism, p. 1–20. Academic, London.

Stolper, E., Walker, D., Hager, B.H., and Hays, J.F. (1981) Melt segregation from partially molten source regions: The importance of melt density and source region size. Journal of Geophysical Research, 86, 6261–6271.

Takahashi, E. (1980) Melting relations of an alkali-olivine basalt to 30 kbar, and their bearing on the origin of alkali basalt magmas. Carnegie Institution of Washington Year Book, 79, 271–276.

Takahashi, N. (1991) Origin of three peridotite suites from Horoman peridotite complex, Hokkaido, Japan: Melting, melt segregation and solidification processes in the upper mantle. Journal of Mineralogy, Petrology, and Economic Geology, 86, 199–215.

——— (1992) Evidence for melt segregation towards fractures in the Horoman mantle peridotite complex. Nature, 359, 52–55.

Takazawa, E., Frey, F.A., Shimizu, N., Obata, M., and Bodinier, J.L. (1992) Geochemical evidence for melt migration and reaction in the upper mantle. Nature, 359, 55–58.

Toramaru, A., and Fujii, N. (1986) Connectivity of melt phase in a partially molten peridotite. Journal of Geophysical Research, 91, 9239–9252.

Vasseur, G., Vernèrs, J., and Bodinier, J.L. (1991) Modelling of trace element transfer between mantle melt and heterogranular peridotite matrix. Journal of Petrology, Special Lherzolites Issue, 41–54.

Waff, H.S., and Bulau, J.R. (1982) Experimental studies of near-equilibrium textures in partially-molten silicates at high pressure. Advances in Earth and Planetary Sciences, 12, 229–236.

Waff, H.S., and Faul, U.H. (1992) Effects of crystalline anisotropy on fluid distribution in ultramafic partial melts. Journal of Geophysical Research, 97, 9003–9014.

Waff, H.S., and Holdren, G.R., Jr. (1981) The nature of grain boundaries in dunite and lherzolite xenoliths: Implications for magma transport in refractory upper mantle material. Journal of Geophysical Research, 86, 3677–3683.

Walker, M.E.L., Jurewicz, S.R., and Watson, E.B. (1988) Adcumulus dunite growth in a laboratory thermal gradient. Contributions to Mineralogy and Petrology, 99, 306–319.

Watson, E.B. (1982) Melt infiltration and magma evolution. Geology, 10, 236–240.

Watson, E.B., and Brenan, J.M. (1987) Fluids in the lithosphere. I. Ex-

perimentally-determined wetting characteristics of CO_2-H_2O fluids and their implications for fluid transport, host-rock physical properties, and fluid inclusion formation. Earth and Planetary Science Letters, 85, 497–515.

Watson, E.B., Brenan, J.M., and Baker, D.R. (1990) Distribution of fluids in the continental mantle. In M.A. Menzies, Ed., Continental mantle, p. 111–125. Clarendon Press, Oxford, U.K.

Wilshire, H.G. (1984) Mantle metasomatism: The REE story. Geology, 12, 395–398.

——— (1987) A model of mantle metasomatism. Geological Society of America Special Paper, 215, 47–60.

Wilshire, H.G., and Kirby, S.H. (1989) Dikes, joints and faults in the upper mantle. Tectonophysics, 161, 23–31.

Wilshire, H.G., and Pike, J.E.N. (1975) Upper-mantle diapirism: Evidence from analogous features in alpine peridotite and ultramafic inclusions in basalt. Geology, 3, 467–470.

Wilshire, H.G., and Shervais, J.W. (1975) Al-augite and Cr-diopside ultramafic xenoliths in basaltic rocks from western United States. Physics and Chemistry of the Earth, 9, 257–272.

Wilshire, H.G., Pike, J.E.N., Meyer, C.E., and Schwarzman, E.C. (1980) Amphibole-rich veins in lherzolite xenoliths, Dish Hill and Deadman Lake, California. American Journal of Science, 280-A, 576–593.

Wilshire, H.G., Meyer, C.E., Nakata, J.K., Calk, L.C., Shervais, J.W., Nielson, J.E., and Schwarzman, E.C. (1988) Mafic and ultramafic xenoliths from volcanic rocks of the western United States. U.S. Geological Survey Professional Paper, 1143, 179 p.

Wilshire, H.G., McGuire, A.V., Noller, J.S., and Turrin, B.D. (1991) Petrology of lower crustal and upper mantle xenoliths from the Cima volcanic field, California. Journal of Petrology, 32, 169–200.

Woodland, A., Bussod, G., Kornprobst, J., Bodinier, J.L., Macpherson, E., and Menzies, M. (1992) The effect of mafic dike emplacement on surrounding peridotite: Evidence from spinel compositions and estimated redox states. Geological Society of America Abstracts with Programs, 24, 85.

Wyllie, P.J. (1978) Mantle fluid compositions buffered in peridotite-CO_2-H_2O by carbonate, amphibole, and phlogopite. Journal of Geology, 86, 687–713.

——— (1979) Petrogenesis and the physics of the earth. In H.S. Yoder, Jr., Ed., The evolution of the igneous rocks, p. 483–520. Princeton University Press, Princeton, New Jersey.

Manuscript received March 23, 1993
Manuscript accepted July 15, 1993